Perceptual evaluation of wind turbine noise

Andrea Bresciani, Julien Maillard, Leandro de Santana

16ème Congrès Français d'Acoustique
11-15 Avril 2022, Marseille

Perceptual evaluation of wind turbine noise

A. P. C. Bresciani [a,b,c], J. Maillard [a], L. D. De Santana [b]

[a] CSTB, 24 Rue Joseph Fourier, 38400 Saint-Martin-d'Hères, France

[b] University of Twente, PO Box 217, Enschede, 7500 AE, the Netherlands

[c] Siemens Industry Software N.V., Interleuvenlaan 68, Leuven, 3001, Belgium

The acoustic impact of wind turbines is currently hampering the societal acceptance and the deployment of green aeolian energy near dwellings. For this reason, an accurate physical and perceptual prediction of wind turbine noise is of crucial importance for the design and deployment of modern horizontal-axis wind turbines. In the present work, we discuss a novel methodology for the far-field propagation and auralization of wind turbine noise in complex rural environments. First, the sound sources are modelled analytically using a RANS-based Amiet's theory, accounting for leading- and trailing-edge noise. Secondly, a geometrical ray-tracing solver is used to compute the multiple source-receiver paths and evaluate the directivity gain. Finally, the Harmonoise ray-based method is used to apply the noise attenuation due to atmospheric absorption, ground barriers, ground effects, and meteorological conditions. This methodology has been applied to the SWT 2.3-93 wind turbine, testing two different ground types for several different receivers. The preliminary results are consistent with previous studies, showing up to 3 dBA of modulation in amplitude for receivers close to the rotor plane. Furthermore, the noise levels in third octave band show that the modulation in amplitude is mainly affecting the medium- and high-frequency ranges.

1 Introduction

Nowadays the deployment of wind turbines near dwellings is limited by their acoustic annoyance. Despite lower noise levels than other environmental noise sources such as wind, road or rail, wind turbine noise has been recognised as the most annoying in several configurations [11]. An extensive review on the adverse health effects caused by wind turbine noise has been published by the Council of Canadian Academics [24], revealing that the evidences are sufficient to establish a causal relationship between wind turbine noise and annoyance. Furthermore, some evidences relate wind turbine noise with sleep disturbances and, indirectly, with stress [24]. For these reasons, wind turbine noise predictions are crucial for the evaluation of their acoustic impact in the surrounding environment.

To predict the noise, two aspects have to be modelled and coupled: the aerodynamic noise sources and the propagation of the sound in the far-field. Several different methodologies have been considered in the past, most of them focusing on the BPM model [4] or Amiet's theory [1, 2] for the noise source modelling, and on the ray-tracing methods [8, 9, 17] and parabolic equation method [7, 23] for the atmospheric propagation. For instance, Cotté [7] coupled Amiet's theory for the prediction of the sources with the parabolic equation method, assessing the validity of the single point source approximation for the wind turbine noise propagation.

In the present work, a RANS-based Amiet's theory for leading- and trailing-edge noise [1, 2] is coupled with engineering ray-based methods, which are able to provide results with the same degree of uncertainty of Amiet's theory and with a computational cost much lower than the parabolic equation or standard ray-tracing. In particular, Harmonoise sound propagation model [21] will be used in this work, but the same methodology can be applied to any other engineering model, such as the ISO9613-2, NMPB-2008, CONCAWE or Nord2000. Thanks to the low computational cost, this methodology can be applied simultaneously to multiple wind turbines in a complex environment, that can potentially include several ground types, buildings and other noise sources such as road or railway traffic.

Preliminary results for the SWT 2.3-93 wind turbine as described in reference [5] are shown for two different ground types and different receivers. The computed time varying noise levels will be used for the calculation of dynamic noise indices as well as the auralization of wind turbine noise in upcoming work. By simulating the pressure time signal at the receiver location, auralization can be used for noise acceptance studies, as well as demonstrators for non-experts, or as a tool for optimal placement of the wind turbines. Different techniques for sampled-based [19] and physics-based [16] auralization have been already applied to wind turbine noise. The present work will contribute further to physics-based auralization of wind turbine. One of the objectives will be to include the proposed techniques to an existing auralization framework for noise annoyance evaluation of complex outdoor sound scenes [13–15].

2 Methodology

The wind turbine blade is divided into segments in the spanwise direction. The aspect ratio of each segment is defiend as $\lambda = L_{\text{span}}/c_{\text{mean}}$, where L_{span} is the spanwise extension of the segment and c_{mean} is the chord length of the airfoil in the middle of the segment. For the SWT 2.3-93 considered, a constant aspect ratio $\lambda = 3$ has been used to satisfy the large aspect ratio assumption of Amiet's theory. The blade segment closer to the root has been enlarged up to $r = 9$ m to include the blade up to the first cross-section with an airfoil shape, resulting in an aspect ratio $\lambda = 4.2$ for this segment. The total number of segments is 6 and they are shown in Figure 1. The airfoil at mid-span of each segment is used in a 2D RANS simulation to compute the boundary layer parameters for the trailing-edge noise Amiet's theory. The angle of attack

of the RANS simulation is computed accounting for the geometrical twist angle of the blade, the collective pitch angle, the velocity triangle formed by the wind speed and rotational speed, and, finally, by the induced angle of attack computed with the momentum theory. For each blade segment, Amiet's theory for leading- and trailing-edge noise is used to compute the noise on the surface of a 1 m radius sphere. These sources are treated as point sources for Harmonoise model [21]. The rotor disk is discretized in the azimuthal direction in 360 stations, resulting in a total of 360x6 sources.

The velocity inflow is assumed constant over the rotor disk resulting in axis-symmetric conditions. This hypothesis allows to drastically reduce the number of RANS and Amiet's theory simulations necessary. It is worth mentioning that the strip theory originally due to Schlinker and Amiet [22] is not used in the present work: the noise levels at the receivers locations are computed using Harmonoise method [21] from the point sources calculated with Amiet's model. The Doppler effect is supposed negligible and will be investigated in future works.

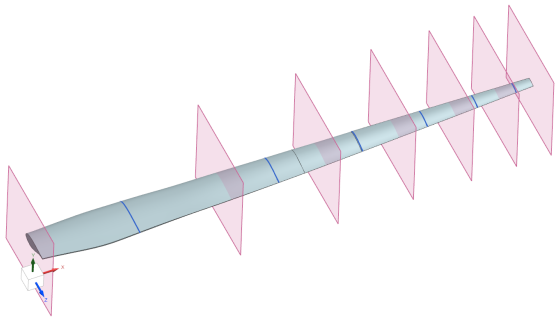

Figure 1: Blade segment decomposition and airfoils used for the 2D RANS simulations (in blue).

2.1 Amiet's model

Leading- and trailing-edge Amiet's theory [1, 2] is used to compute the aerodynamic noise generated by each blade segment. In Amiet's theory, the airfoil is modelled as an infinitely thin flat plate with chord $c = 2b$, span $L = 2d$ and at zero angle of attack with respect to the freestream velocity U. If the observer is located in the acoustic and geometrical far-field and the aspect ratio L/c of the flat plate is large, the power spectral density for trailing-edge noise S_{pp}^{TE} is computed as [20]:

$$S_{pp}^{TE}(\mathbf{x},\omega) = \left(\frac{\omega x_3 b}{2\pi c_0 \sigma_0^2}\right)^2 4d|\mathcal{I}(x_1,k_{10},k_{20})|^2 \\ l_y(k_{10},k_{20})\Phi_{pp}(k_{10},k_{20}), \quad (1)$$

where $\mathbf{x} = (x_1, x_2, x_3)$ is the position of the observer in the reference frame depicted in Figure 2; ω is the pulsation; c_0 is the speed of sound; $\sigma_0 = \sqrt{x_1^2 + \beta^2(x_2^2 + x_3^2)}$; $\beta = 1 - M^2$, M being the Mach number; $\mathcal{I} = \mathcal{I}_1 + \mathcal{I}_2$ is the aeroacoustic transfer function for trailing-edge noise, given in [3, 20]; $k_{10} = \omega/U_c$ with $U_c = 0.7U$; $k_{20} = kx_2/\sigma_0$ with $k = \omega/c_0$; l_y is the spanwise correlation length obtained from Corcos model [6]; Φ_{pp} is the wall pressure spectrum computed with Lee's [12] and Goody's [10] empirical models for computational efficiency. The boundary layer parameters required by the wall pressure spectrum model are computed with 2D incompressible RANS simulations with STAR-CCM+ software.

Amiet's formulation for leading-edge noise reads

$$S_{pp}^{LE}(\mathbf{x},\omega) = \left(\frac{\rho\omega c x_3}{2c_0\sigma_0^2}\right)^2 \pi U d|\mathcal{L}(x_1,k_{10},k_{20})|^2 \\ \Phi_{ww}(k_{10},k_{20}), \quad (2)$$

where ρ is the air density, $\mathcal{L} = \mathcal{L}_1 + \mathcal{L}_2$ is the aeroacoustic transfer function for leading-edge noise [3] and Φ_{ww} is the inflow turbulence spectrum modelled using the von Karman spectrum in this work. The inputs required by the von Karman spectrum are the wind turbulence intensity and integral length scale. Both quantities depend on the location of the wind turbine, the surrounding environment and the time of the day. In this study an integral length scale of 70 m and a turbulence intensity of 20% have been chosen.

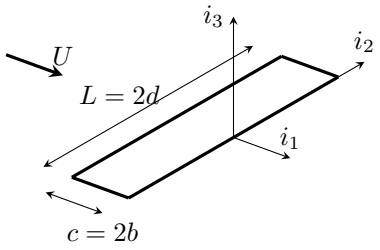

Figure 2: Reference frame for trailing-edge noise.

2.2 Harmonoise model

Harmonoise [21] is an engineering ray-based method used to calculate the sound pressure level at the receiver location in 1/3-octave bands between 50 Hz and 10 kHz, accounting for geometrical attenuation, air absorption and ground reflection. The calculation is composed of two steps. First, a 2D ray tracing is performed in the horizontal plane to account for the different ray paths caused by the reflections due to vertical surfaces. Since, in the present work, no vertical surfaces are considered, only one straight ray path connects the source and the receiver. In the second step, the Harmonoise method is used in the vertical plane containing the source and the receiver. The sound pressure levels $L_{p,ik}$ for a given 1/3-octave band due to the sound source i at the receiver k is computed as

$$L_{p,ik} = L_{w,i} + DI_{ik} - A_{E,ik}, \quad (3)$$

where $L_{w,i}$ is the sound power of the source i, and DI_{ik}, the directivity gain of the sound source i in the direction

of the receiver k. $A_{E,ik}$ is called excess attenuation and collects several terms:

$$A_{E,ik} = [A_{\text{div}} + A_{\text{atm}} + A_{\text{gr+bar}} + A_{\text{sc}} + A_r]_{ik}, \quad (4)$$

which are, respectively, the excess attenuation due to spherical divergence, air absorption, ground (and barrier) reflection and diffraction, scattering by forest and atmospheric turbulence, and, finally, vertical surfaces reflections. In the present work, a simple flat ground with constant absorption coefficient is used. Furthermore, the atmospheric conditions are supposed homogeneous and isotropic, i.e. with zero sound speed gradient.

3 Results and discussion

The operating conditions of the wind turbine are taken from reference [5]: rotational speed RPM = 14, wind speed $W = 8$ m/s and collective pitch angle $\theta = 0$. The wind turbine is placed on a flat ground with constant ground porosity. We will refer to *soft ground* to indicate a ground with porosity $\sigma = 200$ kPa s/m^2, representative of an uncompacted, loose ground, such as grass, and to *hard ground* for a porosity $\sigma = 20000$ kPa s/m^2, representative of asphalt or concrete. Furthermore, a simulation in free-field is also considered for validation purpose. For this simulation only the excess attenuation due to air absorption and spherical divergence is considered.

The noise levels in third octave bands are calculated for 6 receivers at a horizontal distance from the wind turbine $d = 200$ m. One receiver is located downwind at hub-height ($z = 80$ m above ground) for validation purposes: in free-field propagation conditions, the noise levels are not expected to vary because of the axial symmetry of the problem. The other 5 receivers are located at $z = 1.5$ m above ground and placed at 5 different angular positions $\tau = 90°, 70°, 50°, 30°, 10°$, where $\tau = 90°$ is the downwind direction and $\tau = 0$ is the crosswind direction. A schematic of the reference system in the horizontal plane is shown in Figure 3.

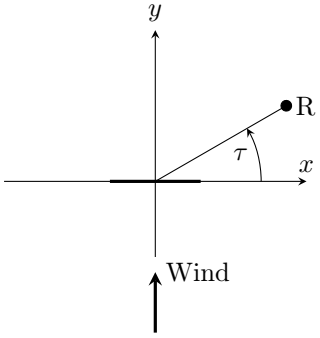

Figure 3: Reference frame for receivers position. The thick segment represents the rotor disk.

Figure 4 shows the results for Overall A-weighted Sound Pressure Level (OASPL) as a function of the azimuthal position of the first blade. The OASPL is computed as the sum of the A-weighted third octave sound pressure levels. It is worth noting that for free-field propagation (Figure 4a), a listener located at hub-height $z = 80$ m would not experience any amplitude modulation, as expected by the axial symmetry of the problem. In general, this is not true when the effect of the ground is included, because the varying source height will introduce an additional amplitude modulation [8]. However, this effect is small for the receivers investigated in this work and, even with a hard ground (Figure 4b), the amplitude modulation is less than 0.1 dB(A). As reported in previous literature, e.g. [7, 16, 18], the OASPL shows amplitude modulations up to 3 dB(A) for receivers close to the rotor plane. If a soft ground is considered (Figure 4c), the total levels decreases by approximately 1.5 dB(A), while the modulation in amplitude is mostly unaffected. It is worth mentioning that the amplitude modulation shown in Figure 4 is caused by the sum of three effects. The first one is the varying relative distance between source and receiver and it is expected to become negligible for receivers far from the wind turbine where the change in the relative distance is negligible. The second effect is due to the directivity of the source model: in the local reference frame of Amiet's theory, the direction source-receiver is not constant with time, causing variation in the noise levels. This effect is expected to be present also at large distances from the wind turbine. The last effect has been discussed above: it is related to the varying source height and its interaction with the reflecting ground.

Figure 5 shows the noise levels in third octave bands for the receiver at $\tau = 10°$, $z = 1.5$ m. The lower limit of the color scale is limited to 10 dB because lower noise levels would not be audible in a real environment with background noise. The amplitude modulation is noticeable for the mid-frequencies and high-frequencies, while, for the 100 Hz central frequency band and below, the amplitude modulation is negligible.

4 Conclusions and future work

In this work, a methodology to couple Amiet's theory for leading- and trailing-edge noise with ray-based engineering models for environmental noise propagation is presented. The results are consistent with previous works from the literature, showing amplitude modulations up to 3 dB(A) in the OASPL for receivers close to the rotor plane. On the contrary, receivers located downwind do not show strong amplitude modulation. Furthermore, it has been shown that the amplitude modulation is mainly related to variations in the medium and high-frequency range.

In future work, the noise will be auralized using

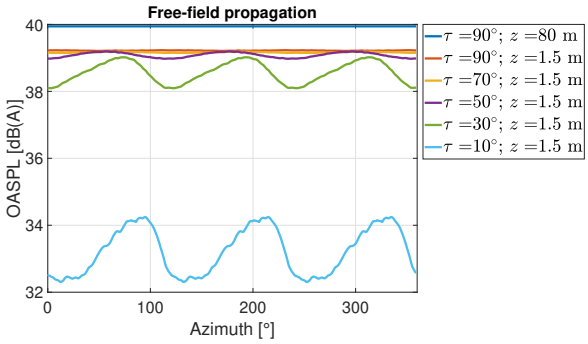

(a)

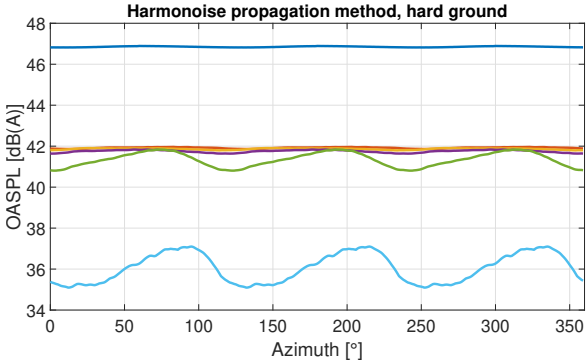

(b)

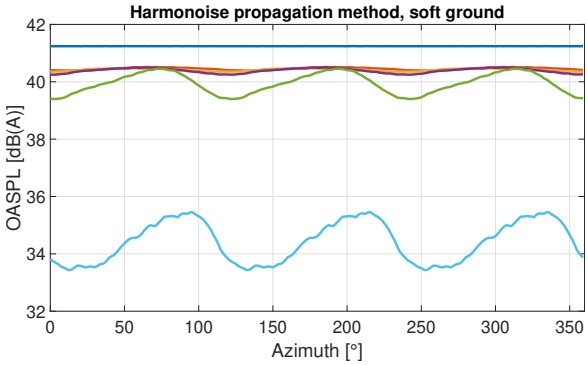

(c)

Figure 4: Overall sound pressure levels in dB(A) for different receiver positions as function of the blades azimuth. (a) Free-field noise propagation: the noise levels are computed considering only the spherical divergence and the air absorption. (b) Propagation with Harmonoise method with an hard ground type (asphalt) and (c) soft ground type (grass).

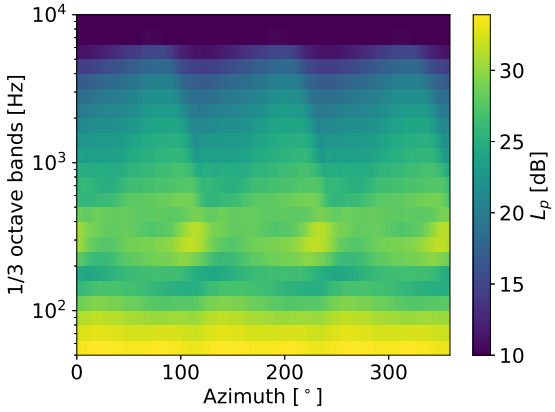

Figure 5: Third octave noise levels for the receiver located close to the rotor plane ($\tau = 10°$ and $z = 1.5$ m).

spectral shaping synthesis coupled with 3D audio rendering of the propagation effects. With the addition of other sound sources, the resulting time pressure signal will be used to evaluate the acoustic annoyance of wind turbine noise in complex environments under different weather and ambient noise conditions.

Acknowledgements

The authors acknowledge the European Commission for its financial support through the H2020-MSCA-ITN-209 project zEPHYR (grant agreement No 860101).

References

[1] R. K. Amiet. Acoustic radiation from an airfoil in a turbulent stream. *Journal of Sound and Vibration*, 41(4):407 – 420, 1975.

[2] R. K. Amiet. Noise due to turbulent flow past a trailing edge. *Journal of Sound and Vibration*, 47(3):387 – 393, 1976.

[3] A. P. Bresciani, S. Le Bras, and L. D. de Santana. Generalization of amiet's theory for small reduced-frequency and nearly-critical gusts. *Journal of Sound and Vibration*, 524:116742, 2022.

[4] T. F. Brooks, S. D. Pope, and M. A. Marcolini. Airfoil self-noise and prediction. Technical report, NASA, Langley Research Center, 1989.

[5] M. Churchfield. A method for designing generic wind turbine models representative of real turbines and generic Siemens SWT-2.3-93 and Vestas V80 specifications. *National Renewable Energy Laboratory, Golden, Colorado*, 2013.

[6] G. M. Corcos. The structure of the turbulent pressure field in boundary-layer flows. *Journal of Fluid Mechanics*, 18(3):353–378, 1964.

[7] B. Cotté. Coupling of an aeroacoustic model and a parabolic equation code for long range wind turbine noise propagation. *Journal of Sound and Vibration*, 422:343–357, 2018.

[8] D. Ecotière. Can we really predict wind turbine noise with only one point source ? In *6th International Conference on Wind Turbine Noise*, number April, Glasgow, 2015.

[9] K. M. Elsen and A. Schady. Different sound source setups in the simulation of wind turbine sound propagation. In *9th International Conference on Wind Turbine Noise*, number May, pages 1–6, Remote from Europe, 2021.

[10] M. Goody. Empirical spectral model of surface pressure fluctuations. *AIAA Journal*, 42(9):1788–1794, 2004.

[11] S. A. Janssen, H. Vos, A. R. Eisses, and E. Pedersen. A comparison between exposure-response relationships for wind turbine annoyance and annoyance due to other noise sources. *The Journal of the Acoustical Society of America*, 130(6):3746–3753, 2011.

[12] S. Lee. Empirical wall-pressure spectral modeling for zero and adverse pressure gradient flows. *AIAA Journal*, 56(5):1818–1829, 2018.

[13] J. Maillard and J. Jagla. Auralization of urban traffic noise - quantitative and perceptual validation. In *Proc. of Congrès Français d'Acoustique (CFA), 22-25 April 2014, Poitiers, France*, 2014.

[14] J. Maillard and A. Kacem. Auralization applied to the evaluation of pedestrian and bike paths in urban environments. In *Proc. of Internoise 2016, Hamburg, Germany, August 21-24*, 2016.

[15] J. Maillard, A. Kacem, N. Martin, and B. Faure. Physically-based auralization of railway rolling noise. In *Proceedings of the 23rd International Congress on Acoustics, 9-13 September, Aachen, Germany*, 2019.

[16] D. Mascarenhas, B. Cotté, and O. Doaré. Physics-based auralization of wind turbine noise. In *9th International Conference on Wind Turbine Noise*, number May, pages 1–6, 2021.

[17] S. McBride, R. Burdisso, and J. D. Parra. An efficient noise modeling tool for wind turbines including sound propagation in arbitrary weather conditions. In *ICSV 2016 - 23rd International Congress on Sound and Vibration: From Ancient to Modern Acoustics*, number April, 2016.

[18] S. Oerlemans and J. G. Schepers. Prediction of wind turbine noise and validation against experiment. *International Journal of Aeroacoustics*, 8(6):555–584, 2009.

[19] R. Pieren, K. Heutschi, M. Müller, M. Manyoky, and K. Eggenschwiler. Auralization of wind turbine noise: Emission synthesis. *Acta Acustica united with Acustica*, 100(1):25–33, 2014.

[20] M. Roger and S. Moreau. Back-scattering correction and further extensions of Amiet's trailing-edge noise model. Part 1: theory. *Journal of Sound and Vibration*, 286(3):477 – 506, 2005.

[21] E. Salomons, D. Van Maercke, J. Defrance, and F. De Roo. The Harmonoise sound propagation model. *Acta Acustica united with Acustica*, 97(1):62–74, 2011.

[22] R. H. Schlinker and R. K. Amiet. Helicopter rotor trailing edge noise. Technical report, National Aeronautics and Space Administration, 1981.

[23] M. Sessarego and W. Z. Shen. Noise Propagation Calculations of a Wind Turbine in Complex Terrain. *Journal of Physics: Conference Series*, 1452(1), 2020.

[24] The Expert Panel on Wind Turbine Noise and Human Health. *Understanding the Evidence: Wind Turbine Noise*. Council of Canadian Academies, Ottawa, Canada, 2015.